Forward-imaging instruments for optical coherence tomography

S. A. Boppart, B. E. Bouma, C. Pitris, G. J. Tearney, and J. G. Fujimoto

Department of Electrical Engineering and Computer Science and Research Laboratory of Electronics, Massachusetts Institute of Technology, Cambridge, Massachusetts 02139

M. E. Brezinski

Massachusetts General Hospital and Harvard Medical School, Boston, Massachusetts 02114

Received July 1, 1997

We discuss the design and implementation of forward-imaging instruments for optical coherence tomography (OCT), which require the delivery, scanning, and collection of single-spatial-mode optical radiation. A hand-held surgical probe for use in open surgery can provide cross-sectional images of subsurface tissue before surgical incisions are made. A rigid laparoscope for minimally invasive surgical OCT imaging provides a simultaneous *en face* view of the area being imaged. OCT imaging is demonstrated on *in vitro* human specimens. © 1997 Optical Society of America

The delivery of optical radiation for medical diagnostic and imaging applications has motivated several unique optical system designs. Forward-imaging devices overcome a limitation of side-imaging devices, permitting data to be collected before the device is introduced into tissue. This concept also permits the image-guided placement of the device in surgery and for monitoring interventional procedures such as tissue incision, resection, and laser surgery. Fiber-optic imaging bundles have been used for forward-imaging endoscopes and catheters and have the advantage of being flexible to permit imaging and beam delivery deep within the body. However, when single-spatial-mode optical radiation is used, as in optical coherence tomography (OCT), significant mode coupling between adjacent fibers can broaden the transverse point-spread function and limit dynamic range.[1] While flexible endoscope- or catheter-based imaging is necessary for internal lumens deep within the body, rigid laparoscopic and hand-held devices are suitable for access to regions during minimally invasive and open-field surgical procedures, respectively.

In this Letter we investigate two instruments for forward imaging, a hand-held probe and a rigid laparoscope. We discuss designs and demonstrate imaging utilizing OCT in *in vitro* human tissue. Optical coherence tomographic imaging is a type of optical biopsy that can image the cross-sectional microstructure of tissue *in situ* and in real time.[2] OCT was orginally applied in ophthalmology for noninvasive imaging of the retinal structure[3] and more recently for imaging highly scattering tissues such as the skin[4] and the vascular system.[5] Previous studies demonstrated OCT imaging using a 1-mm-diameter radial-imaging catheter or endoscope.[6] The combination of OCT with hand-held probe and laparoscopic devices can be a powerful imaging technology for surgery because it permits the cross-sectional imaging of internal tissue microstructure *in situ*. Thus it may be possible to guide surgery near sensitive structures such as nerves and blood vessels[7] and identify abnormal pathology such as the margin between tumor and normal tissue. The hand-held probe and laparoscope are prototypes for the optical design of a general class of OCT surgical imaging instruments.

The principles and physics of OCT were described in Refs. 2 and 3, so only the specific parameters used for our experiments are described here. A Cr^{4+}:forsterite Kerr-lens mode-locked laser with a center wavelength of 1280 nm and a bandwidth of 60 nm is used as a low-coherence light source.[8] Using modest powers of $\sim$5 mW on the specimen yielded sensitivities of 110 dB, corresponding to imaging penetration depths of 2–3 mm in most tissues. Images (2 mm $\times$ 2 mm, 200 $\times$ 200 pixels) were acquired in 15 s. In OCT imaging the beam is directed onto the specimen and images are acquired by measurements of the echo delay of backscattered light for different transverse positions of the OCT beam. The resulting data set is a two-dimensional cross-sectional map of the optical backscattering from the specimen and is displayed as a false-color or gray-scale image. The instrument optics are designed to match the confocal parameter with the depth of imaging penetration.

To perform forward imaging of a single-mode beam, one can translate a lens and (or) a fiber with motors, piezoelectric cantilevers, or elastrostatic or magnetic techniques. A schematic of a piezoelectric cantilever design that translates both a fiber and a gradient-index (GRIN) lens is shown in Fig. 1A. The number of longitudinal backscattering profiles that are acquired during a single transverse scan of the beam determines the number of transverse pixel elements in the OCT image. The relationship between the transverse spot size and the density of transverse pixel elements determines the degree of oversampling or undersampling in the image. To realize full transverse image resolution, one must acquire longitudinal backscattering data with pixel spacing comparable to or less than the transverse spot size. The fiber and

0146-9592/97/211618-03$10.00/0

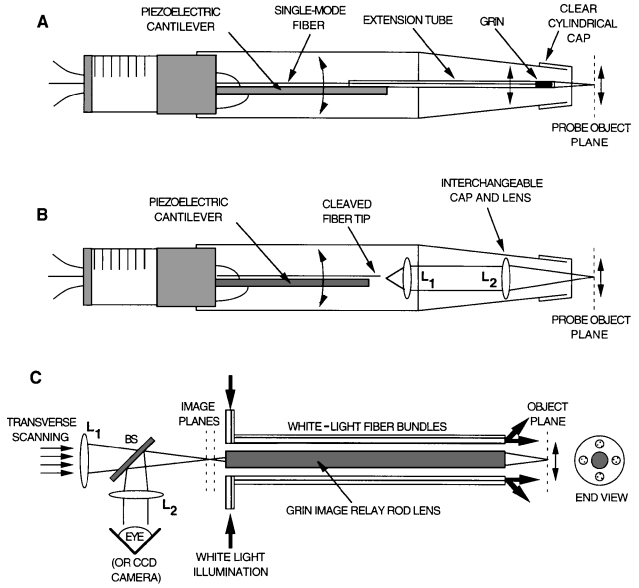

Fig. 1. Schematics of OCT forward-imaging instruments: A, hand-held surgical probe with a piezoelectric cantilever; B, probe telescope design for variable scan length and magnification; C, laparoscope for simultaneous *en face* visualization and cross-sectional OCT imaging. BS, beam splitter.

GRIN design has the advantage that it is a compact single-unit assembly but has the disadvantage of having a fixed magnification.

A second design (Fig. 1B) enables one to vary the magnification by scanning a cleaved fiber tip in the focal plane of the first lens (L_1) in a telescope. The beam is collimated and then focused by a second lens (L_2) that effectively relay images the fiber tip onto the object or specimen. Changing the focal length of the second lens varies the magnification of the scan range in the object plane as well as the optical mode emitted by the fiber tip. Hence, changing the magnification scales both the focused spot size and the transverse scan length congruently, making the ratio of the transverse pixel spacing to spot size constant. Displacement of the fiber tip in the transverse direction results in a transverse displacement of the beam focus in the object plane. The working distance is set by the focal length of the second telescope lens (L_2). The advantages of this design include low mass on the piezoelectric cantilever, permitting higher translation velocities and interchangeable magnification via different lenses.

The hand-held probe design in Fig. 1A was constructed for OCT imaging. A 6.4 mm $\times$ 38.1 mm lead zirconate titanate piezoelectric cantilever (Morgan Matroc, Inc.) was used for transverse scanning. A cantilever displacement of 1 mm was possible with a ramp waveform (0 to 300 V) applied to the cantilever. This displacement was increased to 2 mm by the addition of a 38-mm extension tube to increase the cantilever arm length. The extension tube housed a single-mode optical fiber and a 0.7-mm-diameter, 0.25-pitch, 8°-angle-polished GRIN lens. The GRIN lens was fixed 290 μm from the tip of an 8°-angle-cleaved fiber with UV-cured optical cement. The faces of the GRIN lens and the fiber tip were angled to reduce internal backreflections that would saturate the detector. The faces were oriented parallel to maximize coupling between the optical elements. This produced a 31-μm-diameter spot (the transverse resolution), which corresponds to a 1.2-mm confocal parameter, at a working distance of 3 mm from the GRIN lens. A transparent cylindrical cap of plastic Tygon tubing attached to the end of the probe permitted contact with the tissue and allowed the imaging-beam location on the tissue to be visualized by a coincident visible aiming beam. The cap was replaced after each contact with tissue. The focus of the imaging beam was located at the end of the cylindrical cap.

To demonstrate the imaging capability of the hand-held probe design, *in vitro* images of human ovary and lung (Figs. 2A and 2B, respectively) were acquired with 12-μm axial and 31-μm transverse resolution. The gray scale represents the logarithm of the backscattered light intensity. The images show subsurface morphology of an early primordial ovarian follicle and individual alveoli, which were confirmed with histology and text references. The external surface imaging orientation for the ovary is similar to that encountered during open-field surgical procedures.

In contrast to the hand-held probe used for open-field surgical procedures, rigid laparoscopes permit visualization of tissue at distant (10–50 cm) internal sites while maintaining a small instrument diameter for insertion through small incisions during minimally invasive surgical procedures. A single-rod lens or a series of relay lenses (Hopkins type) can be used for imaging.[9] The laparoscope is especially well suited for OCT imaging because it preserves the transverse-spatial-mode character of the optical beam. It also permits

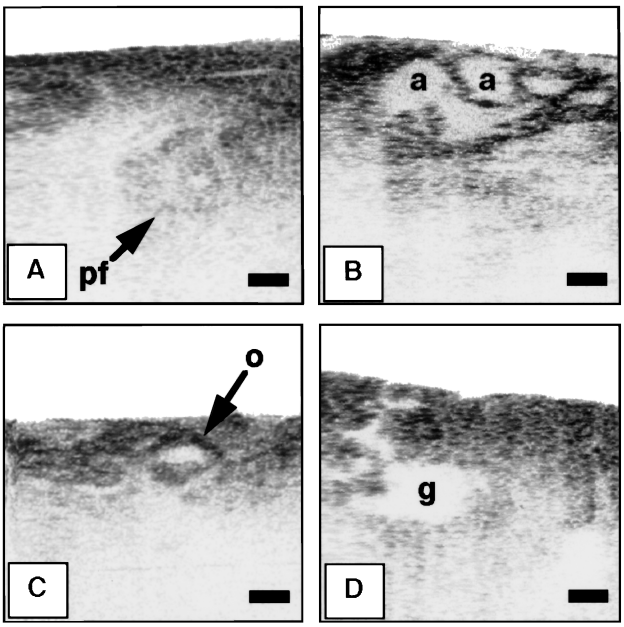

Fig. 2. OCT images of *in vitro* human tissue acquired with forward-imaging instruments: A, ovary with primordial follicle (pf); B, lung alveoli (a's); C, ovary with mature oocyte (o); D, gland (g) in uterus. The bars each represent 250 μm.

simultaneous *en face* imaging of the area being imaged by OCT. One instrument design for a laparoscope is shown in Fig. 1C. A beam splitter and imaging lenses (L_1 and L_2) are incorporated at the proximal end for simultaneous *en face* visualization of the tissue during OCT imaging. White-light illumination fibers are typically located around the perimeter of the rod lens to provide illumination for visualization. The beam scanning at the proximal end can be performed by use of either a piezoelectric cantilever or a galvanometer.

A rigid OCT laparoscope was constructed with a 2.68-mm-diameter 19.5-cm-long rod lens with a nominal pitch length of 3/2 for visible wavelengths. Beam scanning at the proximal end was performed with a piezoelectric cantilever with an attached fiber and GRIN lens, similar to the hand-held probe (Fig. 1A). The index gradient of a rod lens is a function of wavelength, so for 1280 nm the rod pitch length is less than the nominal value of 3/2. Thus an object at a distance of 5 mm from the distal end face of the rod lens yields an image plane at 1 mm from the proximal end face. The focal plane of the piezoelectric-mounted fiber and GRIN lens was placed in the image plane of the rod lens that relay imaged the beam onto the specimen at a working distance of 5 mm from the distal face. A beam splitter was placed between the GRIN and the rod lens to permit the simultaneous visualization of the rod–lens object plane with a CCD microcamera containing a 1/3-in. array. As noted above, because of chromatic dispersion in the rod lens, the image planes for the near-IR and the visible wavelengths are displaced from each other. However, this effect can be compensated for by use of separate focusing elements for the visible beam path and the IR scanning beam path. A 3.6-mm focal-length camera-mounted lens was used as L_2 in Fig. 1C to relay the visible image plane onto the CCD array while the GRIN lens focal plane was placed at the near-IR image plane of the rod lens. Magnification could be adjusted by variation of the positions of the object and the image planes of the rod lens. Alternatively, rod lenses with integral or half-integral pitch lengths could be used with a GRIN objective lens attached directly to the rod lens, either proximally or distally.

Figures 2C and 2D show *in vitro* images of a human ovary and uterus, respectively, acquired with the OCT laparoscope at 12 μm axial and 33 μm transverse resolution (1.3-mm confocal parameter). The imaging orientations are similar to what would be encountered during *in vivo* examination. A gland in the secretory endometrium of the uterus is shown in Fig. 2D and was confirmed with histology. Dynamic *en face* imaging of these specimens provided rapid localization of surface features. When the specimen was positioned at the 5-mm working distance for OCT imaging, the tissue did not have striking surface features within the 2-mm field of view, apart from the location of the coincident visible aiming beam.

The above designs were implemented with a piezoelectric cantilever for transverse scanning because of its simplicity and low cost. The scanning speed is currently limited by the relatively high mass of the cantilever arm and the GRIN lens. However, reducing the mass on the cantilever (Fig. 1B) and tailoring the drive waveform to increase the resonant frequency should make scanning speeds in excess of 100 Hz possible; this is fast enough for real-time imaging applications. With a high-speed OCT system,[10] preliminary studies demonstrating *in vivo* imaging in a rabbit were performed at acquisition rates of 8 frames/s. Scanning can also be performed with galvanometer-driven mirrors, which permit higher scan speeds and three-dimensional imaging but have increased size, cost, and complexity.

In summary, we have presented forward-imaging hand-held probe and rigid laparoscope optical instruments for use with optical coherence tomography. These two devices represent different approaches for OCT imaging and can be powerful diagnostic tools for medical and surgical applications. In future applications OCT imaging might also be integrated with laser-based surgery to permit the simultaneous visualization and surgical incision of tissues on a micrometer scale. Finally, these instrument designs can also be applied to other imaging modalities, such as confocal and multiphoton microscopy, that require the delivery and collection of single-spatial-mode optical radiation.

This research was supported in part by a grant from the U.S. Office of Naval Research, Medical Free Electron Laser Program grant N00014-94-1-0717, National Institutes of Health contracts NIH-9-RO1-EY11289-11 [J. G. Fujimoto (JGF)], NIH-1-R29-HL55686-01A1 [M. E. Brezinski (MEB)], U.S. Air Force Office of Scientific Research grant F49620-95-1-0221, and a grant from the U.S. Air Force Palace Knight Program.

References

1. R. P. Salathé, H. Gilgen, and G. Bodmer, Opt. Lett. **21,** 1006 (1996).
2. D. Huang, E. A. Swanson, C. P. Lin, J. S. Schuman, W. G. Stinson, W. Chang, M. R. Hee, T. Flotte, K. Gregory, C. A. Puliafito, and J. G. Fujimoto, Science **254,** 1178 (1991).
3. E. A. Swanson, J. A. Izatt, M. R. Hee, D. Huang, J. G. Fujimoto, C. P. Lin, J. S. Schuman, and C. A. Puliafito, Opt. Lett. **18,** 1864 (1993).
4. J. M. Schmitt, M. Yadlowsky, and R. F. Bonner, Dermatology **191,** 93 (1995).
5. M. E. Brezinski, G. J. Tearney, B. E. Bouma, J. A. Izatt, M. R. Hee, E. A. Swanson, J. F. Southern, and J. G. Fujimoto, Circulation **93,** 1206 (1996).
6. G. J. Tearney, S. A. Boppart, B. E. Bouma, M. E. Brezinski, N. J. Weissman, J. F. Southern, and J. G. Fujimoto, Opt. Lett. **21,** 543 (1996); erratum, **21,** 912 (1996).
7. M. E. Brezinski, G. J. Tearney, S. A. Boppart, E. A. Swanson, J. F. Southern, and J. G. Fujimoto, J. Surg. Res. **70,** 1 (1997).
8. B. E. Bouma, G. J. Tearney, I. P. Bilinsky, B. Golubovic, and J. G. Fujimoto, Opt. Lett. **21,** 1839 (1996).
9. T. H. Tomkinson, J. L. Bently, M. K. Crawford, C. J. Harkrider, D. T. Moore, and J. L. Rouke, Appl. Opt. **35,** 6674 (1996).
10. G. J. Tearney, B. E. Bouma, S. A. Boppart, B. Golubovic, E. A. Swanson, and J. G. Fujimoto, Opt. Lett. **21,** 1408 (1996).